EI SEVIER

Contents lists available at ScienceDirect

## Surface Science

journal homepage: www.elsevier.com/locate/susc



# Zn effect on STM imaging of brass surfaces



Frédéric Wiame \*, Mazharul M. Islam <sup>1</sup>, Bekir Salgın <sup>2</sup>, Jolanta Światowska, Dominique Costa, Boubakar Diawara, Vincent Maurice, Philippe Marcus

PSL Research University, Chimie ParisTech — CNRS, Institut de Recherche de Chimie Paris, 75005 Paris, France

#### ARTICLE INFO

Article history: Received 17 July 2015 Accepted 17 October 2015 Available online 24 October 2015

Keywords:
Scanning tunneling microscopy
Density functional theory
Friedel oscillations
Chemical contrast
Surface local density of states

#### ABSTRACT

The surface of brass has been characterized by combined experimental and theoretical approaches. The experimental scanning tunneling microscopy study performed on a  $Cu_{0.7}Zn_{0.3}(111)$  surface at room temperature showed terraces of up to several tens of nanometers in width, separated by monoatomic steps. Depending on the tunneling conditions, a disordered pattern or a sharp atomically-resolved hexagonal lattice was observed. The disordered pattern is attributed to the superposition of Friedel oscillations at the surface induced by the presence of Zn atoms. Comparison of simulated images, based on a simple model of randomly distributed point defects, shows a good agreement with experimental results. At atomic resolution, a chemical contrast has been demonstrated between Zn and Cu atoms at the surface showing the random distribution of isolated Zn atoms into the hexagonal lattice.

© 2015 Elsevier B.V. All rights reserved.

#### 1. Introduction

Brass, a Cu-Zn alloy, has been used since the Antiquity for its ease of manufacturing and corrosion resistance. Its properties lead to applications covering the whole range of human activities spanning from plumbing to high technology products. Nowadays, brass is widely used in the radial tires industry in order to enhance the adhesion between rubber and the reinforcing wires [1–4]. Due to this large number of engineering applications, brass has been the subject of much interest for several years [5-7]. However, although it appears as crucial in the understanding of the surface reactivity, very few investigations were dedicated to the characterization of well defined brass single-crystal surfaces [8,9] and almost none was performed at the nanometric scale [10]. Scanning tunneling microscopy (STM) results have been obtained for Zn deposited on Cu(111) surfaces [11]. In this case, the authors observed surface alloying and the STM images suggested that the Zn atoms were randomly distributed into the Cu substrate. Hammer [12] showed by Auger Electron Spectroscopy, using principal component analysis and target factor analysis methods, that the Zn surface concentration may differ from the bulk composition on brass polycrystalline samples. This author evidenced that, for Zn contents ranging from 0% to 48 at.%, the composition is different at the surface and that the surface Zn concentration equals half the bulk one.

In this paper, we report on a joint experimental and theoretical investigation of the atomic structure of a CuZn single-crystal surface. The brass surface was characterized by STM and the corrugation observed at the nanometer scale was explained by a simple point defect model superposing Friedel oscillations. The chemical contrast observed at the atomic scale was simulated using a periodic density functional theory (DFT) approach. To our knowledge, this is the first report of a combined experimental and modeling study of the effect of Zn atoms on the STM imaging of a brass surface.

#### 2. Methods

#### 2.1. Experimental details

The surface of the (111)-oriented  $Cu_{0.7}Zn_{0.3}$  single-crystal (Surface Preparation Laboratory) was mechanically polished with diamond spray with a final grade of 0.25  $\mu$ m and then annealed at 520 K for two hours under a flow of ultra-pure (6N) hydrogen at atmospheric pressure. Higher annealing temperatures were avoided as they induce noticeable dezincification of the sample [10]. The experiments were performed in an ultra high vacuum (UHV) system (base pressure below  $10^{-10}$  mbar) equipped with a STM (Omicron) and with facilities for Auger Electron Spectroscopy (AES), Low Energy Electron Diffraction (LEED) as well as sputtering and annealing of the sample. The brass surface was prepared by repeated cycles of sputtering ( $P_{Ar} = 1 \times 10^{-5}$  mbar, 500 V,  $1 \mu A/cm^2$ ) and annealing (400 K) until a sharp (1 × 1) LEED pattern was observed and no contamination was detected in the AES spectrum. In these conditions, increasing the temperature above 400 K induces a very fast dezincification over several hundreds of nanometers under the

 $<sup>* \ \</sup> Corresponding \ author.$ 

E-mail address: frederic.wiame@chimie-paristech.fr (F. Wiame).

<sup>&</sup>lt;sup>1</sup> Present address: Mulliken Center for Theoretical Chemistry, Institute for Physical and Theoretical Chemistry, University of Bonn, Beringstrasse 4, 53115 Bonn, Germany.

<sup>&</sup>lt;sup>2</sup> Present address: Tata Steel, Research & Development, P.O. Box 10.000, 1970 CA muiden, The Netherlands.

surface, as evidenced by scanning electron microscopy in energy dispersion mode, and confirmed by the sample's color change.

All the presented STM images were recorded at room temperature in constant current mode. Positive bias voltages correspond to empty-state images. No filtering was used. Background plane subtraction was applied and linear drift correction was performed when needed.

#### 2.2. Computational details

The theoretical investigation on Cu(111) and Zn-enriched Cu(111) surfaces was performed by periodic DFT calculations. The GGA-based Perdew–Burke–Ernzerhof (PBE) exchange-correlation functional [13] was employed using VASP [14–16]. The projector-augmented wave (PAW) potentials [17,18] were used for the core electron representation, whereas the valence electrons were represented by the energy cutoff  $E_{\rm cut}=360$  eV as converged for the bulk Cu optimization in the present study. The integration in reciprocal space was performed on a Monkhorst-Pack grid [19]. The convergence of bulk properties was checked with increasing k-point grids. Based on the optimized bulk structure (optimized lattice parameter, a=0.363 nm), a  $(2\times 2)$  supercell was constructed for the Cu(111) surface with increasing number of Cu layers. A vacuum layer of 1.5 nm along the z direction perpendicular to the surface (x and y being parallel to the surface) was employed to prevent interactions between the repeated slabs.

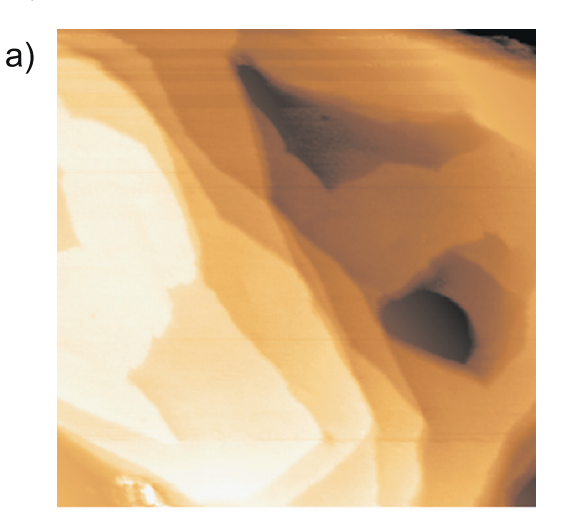
For electronic properties analysis, local density of states (LDOS) calculations were performed for optimized slabs with an increased k-points grid (8  $\times$  8  $\times$  1). STM images were simulated using the Tersoff–Hamann [20] approach which provides a reliable qualitative picture of the surface topography. In this method, the surface is treated exactly, while the tip is modeled as a locally spherical potential well. The tunneling current is proportional to the surface LDOS at the position of the STM tip. Similar approach was employed for the DFT STM simulation on the TiAl(111) surface [21].

For the calculation of atomic charges, we have used the "Bader" code developed by Henkelman et al. [22] which implement the Bader's method in which atomic charges are calculated using the decomposition of electronic charge density into atomic contributions by dividing the space into atomic regions with surfaces at a minimum in the charge density.

### 3. Results and discussion

As mentioned, the annealing temperature is limited by the dezincification of the sample under UHV conditions. This is a major problem for the preparation of well-organized flat surfaces needed for high resolution STM measurements. This may partly explain why so few near-field studies have been performed on such single-crystalline samples. Moreover, the surface obtained after long-lasting preparation still presents many hills and valleys at the nanometer scale (Fig. 1a), which makes it difficult to obtain atomic resolution. However, one can identify monoatomic steps on the substrate (0.21 nm high). The width of the terraces can reach several tens of nanometers. On Fig. 1b, several defects (screw dislocations) present at the surface are circled out. They probably result from the annealing temperature limitation.

For certain tunneling conditions (associated with large tip-surface distances compared to atomic resolution conditions), oscillations (corrugation of 0.04 nm) forming a disordered pattern on the clean terraces are observed (Fig. 2a, showing also a screw dislocation). We will show that these features can be explained by electronic effects. Indeed, as observed on Cu(111) surface with adsorbed oxygen atoms at room temperature [23], a local perturbation of the electron density may generate oscillations in the electrostatic potential, known as Friedel oscillations [24], which induce electron standing wave patterns at the surface. The perturbation of the



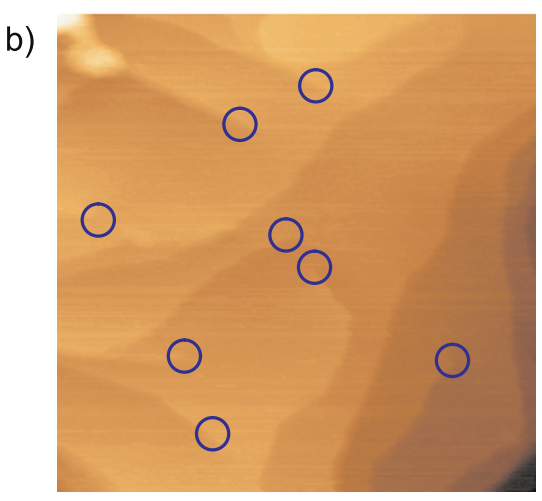


**Fig. 1.** STM images a) 100 nm  $\times$  100 nm, V=0.5 V, I=0.5 nA, b) 80 nm  $\times$  80 nm, V=0.7 V, I=0.2 nA, of the clean  ${\rm Cu_{0.7}Zn_{0.3}(111)}$  surface. The emergence of screw dislocations is circled in b).

LDOS around a point defect in a two-dimensional electron gas is proportional to

$$\Delta \rho \propto J_0(kr) Y_0(kr) \tag{1}$$

where  $J_0$  and  $Y_0$  are the zero-order Bessel functions of the first and second kind, respectively, r is the distance to the defect and k the wave vector. The asymptotic behavior for  $kr \gg 1$  is given by

$$\Delta \rho \propto \frac{\cos(2kr)}{kr}.\tag{2}$$

The tunneling current may be calculated by integrating the LDOS over the all range of energies between  $E_F$  and  $E_F + eV$ . The measured height z in constant current mode can thus be extracted taking into account the fact that the tunneling current  $I \propto \exp(-\kappa z)$  where  $\kappa$  essentially depends on the work functions of the tip and sample.

At finite temperature, another attenuation term with the distance to impurity has to be taken into account. The temperature effect can be approximated by multiplying the results at 0 K by a function  $\beta r/\sinh(\beta r)$  [25,26] where

$$\beta = \frac{2\pi m^*}{\hbar^2} \frac{k_B T}{k}.\tag{3}$$

This attenuation term is close to 1 in the vicinity of the impurity and varies as  $2\beta r \exp(-\beta r)$  for  $\beta r \gg 1$ . This explains why it is more

# Download English Version:

# https://daneshyari.com/en/article/5421565

Download Persian Version:

https://daneshyari.com/article/5421565

<u>Daneshyari.com</u>